Hydrogeology Journal   Springer

A Structural and Geophysical Approach to the Study of Fractured Aquifers in the Scansano-Magliano in Toscana Ridge, Southern Tuscany, Italy

scholarONE™
Manuscript Central

Francese et al., 2007

A Structural and Geophysical Approach to the Study of Fractured Aquifers in the Scansano-Magliano in Toscana Ridge, Southern Tuscany, Italy

Roberto Francese[1], Francesco Mazzarini[2], Andrea Bistacchi[3], Gianfranco Morelli[4], Giorgio Pasquarè[5], Nicola Praticelli[6], Henry Robain[7], Nigel Wardell[1] and Annalisa Zaja[6]

[1] Istituto Nazionale di Oceanografia e di Geofisica Sperimentale, Trieste, Italy

[2] Istituto Nazionale di Geofisica e Vulcanologia, Pisa, Italy

[3] Dipartimento di Geologia e Geotecnologia, Università di Milano Bicocca, Milano, Italy

[4] Geostudi Astier S.r.l., Livorno, Italy

[5] Dipartimento di Geologia, Università di Milano, Milano, Italy

[6] Dipartimento di Geoscienze, Università di Padova, Padova, Italy

[7] Institute de Recherche pour le Développement, Paris, France

Corresponding Author

Francesco Mazzarini**,** Istituto Nazionale di Geofisica e di Vulcanologia, Via della Faggiola 32, 56126, Pisa, Italy. Phone: 0039 0508311956, Fax: 0039 0508311942, e-mail: mazzarini@pi.ingv.it

ABSTRACT

Fresh water availability has recently become a serious concern in the Italian Apennines, as various activities rely on a predictable supply. Along the Scansano-Magliano ridge in southern Tuscany the situation is further complicated by contamination of the nearby alluvial aquifers. Aquifers locally consist of thin fractured reservoirs, generally within low-permeability formations, and it can be difficult to plan the exploitation of resources based on conventional techniques. An integrated study based on geological investigate the link between tectonics and groundwater circulation and to better define the hydrological model. After the regional identification of fault and fracture patterns, a major structure was investigated in detail to accurately map its spatial position and to understand the geometry and properties of the associated aquifer and assess its exploitation potential. The subsurface around the fault zone was clearly imaged through Ground Probing Radar, 2D and 3D resistivity tomography, and 3D shallow seismic surveys. The vertical and horizontal

1

Francese et al., 2007

contacts between the different geological units of the Ligurian and Tuscan series were resolved with a high

degree of spatial accuracy. 3D high-resolution geophysical imaging proved to be a very effective means for

characterising small-scale fractured reservoirs.

Key Words: southern Tuscany, fractured rocks, geophysical methods, tectonics, groundwater exploration.

2

Francese et al., 2007

INTRODUCTION AND MOTIVATION

In the last decades the problem of fresh water supply has been dramatically amplified by the progressive growth of human activity and by intensive land use, with important implications for water resource exploration and exploitation. Water resource management is becoming of crucial importance throughout the world, especially in areas such as the Mediterranean characterised by long dry or arid seasons and very short rainy periods. At the same time, "per capita" water consumption is growing constantly; in Italy this consumption has been recently estimated to be about 250 l per day (Legambiente, 2003). Although tourism and high quality agriculture can play a major role in the sustainable development of central Italy, by attracting investments and generating profits, this socio-economic model results in the scattering of many different human activities over wide areas. In order to assist such development, Regional Administrations and National Institutions should establish an effective network for the exploitation and distribution of water resources.

Local aquifers in the Tuscan Apennines generally consist of thin fractured reservoirs, often within low-permeability formations. Due to their complex geometry these aquifers can be very difficult to identify and map using the classic techniques; nevertheless, they may represent a series of small-scale water reservoirs of great interest to local economies.

A modern approach to understanding the implications of the geometry, distribution and status of the fracture network in water circulation should be based on a detailed study of the geology of the area. Geology represents the basis for the effective study and management of water resources. Also note that the hydrological balance is somewhat geology-dependant (it is related to bedrock stratigraphy and lithology, fracture and fault systems, quaternary coverage, etc.) and that regional permeability estimates are often based on outcropping lithologies.

Based on the above considerations, the full characterization of a fractured aquifer involves two major steps: first the definition of the geometry of fault planes and, second, the hydraulic parametrization of the rock body in which water circulation occurs. This study mainly focuses on the first step, deferring to further experiments for the collection of detailed information about aquifer permeability and transmissivity. This work describes the results of a comprehensive structural geology and geophysical survey conducted along

3

the "Patrignone Fault Zone", in the Scansano-Magliano in Toscana Ridge between the Ombrone and Albegna rivers, in order to define the fault zone architecture and permeability structure (Figure 1a).

The geological survey of the study area was first performed in terms of lithological and fracture mapping to define the location of major faults. Geophysical methods were subsequently used to better locate the detected faults and to image their geometry at depth (about 100 m).

Several studies have reported on the geological and geophysical imaging of near surface faults (Demanet et al., 2001; Nguyen et al., 2005; Wise et al., 2003) and on the characterisation of fractured aquifers (Porsani et al., 2005; Sharma and Baranwal, 2005). This paper reports on the geological survey and geophysical imaging of such faults, completed as a first step in the assessment of the fresh water potential of the Fosso Patrignone area. Results were used to formulate a preliminary conceptual model for the structural and hydraulic framework of the Fosso del Patrignone Fracture zone.

GEOLOGICAL OUTLINE AND LOCAL SETTINGS

Southern Tuscany represents an inner portion of the northern Apennine chain characterised by eastward nappe stacking (Boccaletti et al., 1971). The nappe pile is characterised by oceanic units (Ligurian Units l.s.) thrust above the sedimentary and/or low-grade metamorphic sequences of the continental units (the Tuscan Nappe Unit), with low-grade metamorphic rocks locally representing the pre-Alpine basement (Bertini et al., 1991; Decandia et al., 1998). Continental and marine deposits (the "Neoutoctono cycle"; Bossio et al., 1993) cover the nappe stack unconformably. As in other portions of the northern Apennine chain, two main tectonic phases have been identified in southern Tuscany (Carmignani et al., 1995). The first tectonic phase, of Late Oligocene – Lower Miocene age, corresponds to crustal shortening and thickening. It led to the development of east-facing folds, thrusts and nappe structures, with the overthrusting of Ligurian Units onto the Tuscan Nappe. During the second tectonic phase, extensional tectonics affected the chain at different times. Early - middle Miocene extension developed by means of low angle detachment faults as consequence of upper crust delamination (Bertini et al., 1991; Bartole, 1995; Carmignani et al., 1995). Starting in the Late Miocene, the northern Tyrrhenian Sea and southern Tuscany were affected by widespread magmatism (Innocenti et al., 1992; Serri et al., 1993). The outlined stratigraphic and tectonic setting of southern Tuscany highlights the complex tectonic evolution of the area starting in the early-middle Miocene. It is evident that

Francese et al., 2007

such a complex Neogene tectonic evolution, also characterised by important uplift of Pliocene continental deposits up to 600 m a.s.l. (Pasquarè et al., 1983; Marinelli et al., 1993), led to the development of both shallow and deep fracture systems that probably strongly control water circulation.

The Scansano – Magliano in Toscana Ridge

The Scansano – Magliano in Toscana Ridge (SMTR) is located close to the Tyrrhenian coast of southern Tuscany. It is formed by several topographic highs extending from the Ombrone River in the north to the Albegna River in the south (Figure 1a, b). In the SMTR the Ligurian Units l.s. (L) consist of an ophiolite sequence (middle - upper Jurassic) covered by chert (upper Jurassic) and by lower Cretaceous pelagic sediments; the sequence ends with upper Cretaceous – Eocene flysch. Ligurian Units overlie the upper portions of the Tuscan Nappe sequence (T) consisting of pelagic deposits (lower Jurassic – Oligocene) covered by upper Oligocene – lower Miocene syn-orogenic foreland deposits (Benvenuti et al., 1971; Burgassi et al., 1983; Bonazzi et al., 1992; Decandia et al., 1998).

The main lithology in the SMTR consists of upper Oligocene – lower Miocene sandstones and siltstones (Macigno Formation) forming the upper part of the Tuscan Nappe sequence (e.g. Burgassi et al., 1983). The clay-dominated deposits of the Ligurian Units tectonically overlie the sandstones. This stack was subsequently affected by brittle deformation, with the development of N-S and NNW-SSE fault systems; minor E-W and NE-SW trending faults and fractures also developed (Zanchi and Tozzi, 1987; Martelli et al., 1989). One of the major N-S structures lies along the Fosso Patrignone Stream, a few kilometres west of Scansano (Figure 1a).

The Fosso Patrignone Fault Zone

The SMTR structure is essentially controlled by high angle N-S faults. A fracture zone 2-3 km wide and about 12 km long was identified along the Fosso Patrignone Stream (Figure 1a). Geological mapping, structural analysis and geophysical prospecting were completed in order to define the hydrologic potential of the Fosso Patrignone Fault Zone (PFZ).

Four main lithostratigraphic units were identified along the PZF and mapped (Figure 2a). The youngest mapped unit consists of alluvial and colluvial deposits, soils and regolith cover. Quaternary travertine deposits also belong to this unit. The Neogene unit consists of clays and sandy clays (Pliocene) and of conglomerates and sandstones (upper Miocene). Along the PFZ the Tuscan Nappe Unit consists of

5

sandstones and siltstones (Macigno Formation, upper Oligocene – lower Miocene) and of marls, clays, siltstones and calcarenites (medium-upper Eocene). The Ligurian Unit consists of greywackes (Pietraforte Formation, medium-upper Cretaceous) and of clays and limestones (Paleocene – Eocene).

Permeability is highly variable in the lithologies mapped along the PFZ (clay and shale, sandstone, siltstone, limestone, gravel and sand), with values ranging from 10^{-20}-10^{-17} m^2 in shale to $10^{-12} – 10^{-8}$ m^2 in gravel and sand (e.g. Schon, 2004). It is generally possible to group the identified lithologies into four hydrogeologic units:

- The first unit consists of alluvial deposits, sand and travertine and is characterised by medium to high permeability;

- The second unit is composed of sandstones (mainly Macigno Formation and to a lesser extent Pietraforte Formation) and a few landslide deposits. This unit is considered to have medium to low permeability;

- The third unit consists of clays, siltstones and marls (mainly Ligurian Units) and has low to very low permeability;

- The fourth unit, composed of Pliocene clays, is considered impermeable.

Remarkably, all the productive wells are located close to the main fault of the PFZ (easternmost fault in Figure 2a).

FRACTURE ANALYSIS AND PERMEABILITY STRUCTURE

Channelized flows are characteristic of fractured rocks, where fractures give rise to a secondary permeability several orders of magnitude greater than the permeability of intact rock volumes. The hydraulic behaviour of fractures depends on their architecture, geometric features, attitude, distribution and connectivity (e.g. Caine et al., 1996; Margolin et al., 1998; Darcel et al., 2003).

Several fractures and faults were measured along the PFZ (Figure 2c); their azimuth distribution shows major NNW-SSE, N-S and E-W trends (Figure 2c). This distribution of fractures is consistent with geologic observations along the PFZ (Figure 2a), indicating that E-W trending strike slip faults connect sectors of the generally N-S trending fault zone. Note that several productive wells as well as a number of active springs are present in the PFZ area; they are located on a topographic high close to the major faults in the area (Figure 2a). On the basis of these observations, four sites along the PFZ were selected for further

6

Francese et al., 2007

investigation (Podere Aione, Podere Giaggioli Alti, Ripacci and Il Poderino; Figure 3) according to the

modalities and codes listed in Table 1. The sites are mainly located on the western side of the PFZ, where the

highest density of wells and springs has been observed. Three trenches were excavated along the mapped

PFZ (about 12 km long), where the fault zone juxtaposes the sandstones of the Macigno Formation with the

terrains of the Ligurian Units (mainly clays and minor limestone lenses).

Trenches are spaced about 1-2 km apart along the strike of the PFZ. They are about 1-1.5 m deep and about

10-15 m long; the fault juxtaposing the sandstones (Macigno Formation) with the clays and limestones

(Ligurian Units) was intercepted in each trench. Fault zones generally have steep dip angles ranging from

65°to 80°, with the development of damaged zones characterised by open, steeply dipping fractures and by

fault core zones locally marked by metre-thick fault gouge (Figure 4a). The thickness of the fault zone,

damage zone, and fault core have been measured along three sections in each trench (Table 2).

The original tectonic contact which juxtaposes the Ligurian Unit with the sandstones of the Tuscan Nappe

sequence (Carmignani et al., 1995) was reactivated by normal faulting forming the N-S structures as well as

the PFZ.

The architecture of a fault zone strongly controls its permeability structure (Caine et al., 1996). The fault

core (the most highly deformed zone of the fault in which fault gouge and clay-rich materials develop) seals

the fault and acts as a barrier to fluid circulation. Moving away from the fault core, an area of less intense

deformation develops: the damage zone, in which fracture formation enhances rock permeability (e.g. Caine

et al., 1996). According to Caine et al. (1996), the total width of a fault zone (Fzw) can be divided into a core

zone (Fc) and a damaged zone (Fd). Using these simple geometric parameters, it possible to define the *Fa*

ratio (*Fd/Fzw*). The higher the *Fa* value (> 0.5-0.6), the higher the permeability of the fault zone. *Fm* is an

average estimation of *Fa,* and *Fs* is the difference between the maximum and minimum *Fa* values (e.g.

Caine et al., 1996). According to Caine et al. (1996), fault zones that are dominated by damaged zones (i.e.

with high *Fm* values) tend to form in clastic rocks.

The surface and near surface (i.e. in trenches) observations of the fault zone architecture are only a proxy for

the hydraulic properties of the fault zone at depth. The increase in lithostatic load at depth clearly influences

the permeability of the fault zone. We assume that the observed relative proportion of damaged zones and

core zones in the fault zone are representative of the whole fault.

Francese et al., 2007

The PFZ shows a variable geometric parameters (Fm values), with Fc values ranging from a few decimetres to several meters (average of 2.29 m; Figure 4c). The Fd has an average value of 9.78 m. The fault zone width averaged over the three trenches is 12.07 m. Rocks with different permeability are in contact along the PFZ, and the overall fault architecture (generally Fa values higher than 0.5, Caine et al., 1996) indicates the occurrence of a higher permeability damage zone in the fault zone. The "Podere Aione" and "Il Poderino" sites have the highest *Fa* values (Table 2). According to Caine et al. (1996), the relatively low *Fs* value (0.35) for the PFZ suggests that the fault zone has a relatively uniform fault architecture. The favourable permeability structure of the PFZ revealed by trench analysis agrees with the abundance of productive wells along the fault zone. The highest *Fm* value (0.95) at the Poderino site is consistent with the observed high concentration of productive wells (Figure 2a).

GEOPHYSICAL FRAMEWORK

Available data and the strict spatial correlation between the location of productive wells and the occurrence of faults in the PFZ (Figure 2a) suggest that water circulation is strongly controlled by fractures (very thin, nearly vertical aquifers). The exploitation of these aquifers requires a detailed, clear understanding of their geometry (Taylor et al., 1999), as even small (few degrees) variations in the spatial orientation of the fault plane, especially at shallow depths, may result in the drilling of dry wells (Figure 4b).

For this reason, an experimental geophysical exploration campaign was undertaken with the aim of assessing the most suitable techniques (in terms of resolution and cost-effectiveness) for determining the spatial position and thickness of the fault zone.

GEOPHYSICAL DATA ACQUISITION AND PROCESSING

Four geophysical surveys were conducted at three distinct sites ("Aione", "Ripacci" and "Poderino") along the PFZ. Ground Penetrating Radar (GPR) and Earth Resistivity Tomography (ERT) profiles were collected during autumn 2003 and early winter 2004. A 3D-ERT survey was carried out in summer 2004, whereas a 3D seismic survey combining refraction tomography and reflection techniques was undertaken during spring 2005. The chronology of geophysical campaigns is reported in table 3.

8

Francese et al., 2007

Field measures

At the "Aione" site we collected three ERT profiles using both Wenner and dipole-dipole configurations, with 2.0 m and 3.0 m electrode spacing and a series of GPR scans (Figure 5a and Table 3). Two different resistivity meters were used: a 48-electrode IRIS Syscal R1 and a 64-electrode proprietary system of the University of Padova. Radar data were collected with a GSSI Sir System 2000 equipped with a 200 MHz antenna.

At the "Ripacci" site we only collected GPR data using a GSSI Sir System 2000 equipped with a 400 MHz antenna (Figure 5b and Table 3).

At the "Poderino" site we focused on geophysical data acquisition, as the contact location was known through previous trench excavation and the gently dipping morphology made the site particularly accessible; we tested and compared a variety of different techniques and data collection schemes (Figure 5c and Table 3), including 3D measures.

Early tests indicated that the Ligurian and Tuscan Units could be successfully differentiated in terms of terrain resistivity, suggesting that, with respect to GPR data, electrical images would be better suited for mapping tectonic contacts. Even after data processing, radar imaging of the fractured zones generated poor quality sections probably due to the presence of clay minerals in the Ligurian Units and to the high conductivity of the fractured zones, which greatly attenuated the reflected signal.

At this site we collected four ERT profiles with a 48-electrode IRIS SYSCAL PRO device using both Wenner and dipole-dipole configurations (Figure 6a). Electrode spacing was set respectively to 10.0 m in profile ERT-3 (470 m), to 3.0 m in profiles ERT-4 and ERT-5 (141 m), and to 2.0 m in profile ERT-6 (94 m). During the first campaign an additional, more detailed (1.0 m station spacing) profile (ERT-0c) was also collected roughly in the same position as ERT-4 using a 64-electrode proprietary resistivity meter.

Three-dimensional ERT data were collected with a 192-channel SYSCAL PRO system on a 5.0 x 5.0 m square grid (Figure 6b). A total of 288 electrode stations along 12 lines, plus two infinite electrodes, were laid out in the field, and 30200 data points were collected using the pole-pole, pole-dipole and dipole-dipole arrays (Figure 6b).

The most recent survey, a 3D seismic investigation of an area measuring approximately 200 m x 170 m (Figure 7), aimed to map the fault zone at greater depth and to compare the resolution capability of resistivity

9

and seismic data. Seismic data were collected using four "DMT Compact" modules, three "SEISTRONIX-RAS-24" units, and two seismographs ("GEOMETRICS Strataview" and "ABEM Terraloc"), for a total of 216 live channels. Receivers were laid down along nine 24-channel lines with an inline spacing of 5.0 m and a crossline spacing of 10.0 m. A 14-Hz vertical sensor was placed at each geophone station.

Source stations were distributed on a square grid with 10m spacing, and 316 shots were recorded (Figure 7). Elastic energy was propagated into the ground with a silenced 8-caliber rifle.

Data analysis and processing

Only the radar signal recorded in the "Ripacci" site profiles could be used; data from the "Aione" and "Poderino" sites were of extremely poor quality because of the high soil conductivity. Data were processed using the open source Colorado School of Mines, Center for Wave Phenomena (CSM-CWP) Seismic-Unix (SU) package running on a Sun Solaris operating system in a microcomputer-based environment. The processing flow was quite straightforward and included zero-offset correction, background removal, band pass filtering, horizontal filtering, amplitude recovery and migration. A running average filter (Daniels, 1996) was applied to remove the DC signal component.

ERT data from both the "Aione" and Poderino" sites was of very good quality. Pre-processing consisted in noise removal and assigning field geometry. Data inversion from apparent to true resistivity was carried out with the RESINV 2D/3D and OHMVision (distributed by Geostudi Astier) software packages. A rapid convergence of the model response to field data was always observed during the inversion process, and the RMS error was always lower than 10%.

At these two sites we observed very good agreement between the Wenner and dipole-dipole configuration results. Although the dipole-dipole method provided a better image of the vertical contact, we preferred the Wenner method because of its greater penetration depth and the reduced rms error in the inversion process.

The 3D resistivity volume clearly revealed a decrease in the signal-to-noise ratio at a depth of more than 35-40 m from the surface. Although the field configurations used for data acquisition (pole-pole, pole-dipole and dipole-dipole) generated impressive images of the uppermost layers, they have an intrinsically low signal strength. The maximum order of aperture of the different dipoles was optimized prior to data acquisition, but it was impossible to take into proper account local variability in current pathways. For the above reasons, the bottom part of the 3D resistivity volume is not fully reliable for geological interpretation.

10

Francese et al., 2007

The recorded seismic data were generally of good quality; the first breaks were marked and easy to pick out, even at larger offsets. First break picking was carried out manually in order to fully control data quality and consistency. A total of 61200 travel-times were selected and pre-processed prior to 3D refraction tomography inversion. Inversion was carried out with the Pavel Ditmar and Yuri Roslov FIRSTOMO commercial package (distributed by Europex) and with the OGS CAT3D research software (distributed by Paneura - http://www.3dtomography.com). A ray-tracing solution, based on diving waves, was computed over a cubic grid with 5 m spacing. It took approximately 3 hours per run to complete inversion on a parallel cluster of ten 2.8 GHz PIV personal computers.

RESULTS AND DISCUSSION

The "Aione" site

Geological evidence indicates that at this site the PFZ is represented by two parallel structures, and the major tectonic contact appears to coincide with the eastern fault (Figure 5a).

Resistivity sections (Figure 8), exhibit values ranging from 10 ohm*m to about 700 ohm*m. According to surface observations, the resistivity of Tuscan Units (T) is generally greater than 150 ohm*m, while that of the Ligurian Units (L) ranges from 10 ohm*m to about 60-90 ohm*m.

The northern profiles (ERT-1 and ERT-0a), collected using the Wenner configuration, clearly mark the vertical boundary between a resistive domain and a conductive one (at X=120 m in ERT-1 and at X=48 m in ERT-0a). The boundary is sub-vertical and in good agreement with the geological map (Figure 5a), where a fault structure with this orientation is expected in this position. A second vertical boundary, marked by a sudden increase in conductivity, is visible within the resistive domain (at X=84 m in ERT-1 and at X=24 m in ERT-0a). This second boundary corresponds to the one visible in the geological map (Figure 8).

The geophysical image is not as clear in profile ERT-2, although two vertical contacts between conductive and resistive domains are visible on the eastern side of the profile (Figure 8). In this case there is no corresponding feature in the geological map (Figure 5a), as the two tectonic structures of the PFZ appear to be shifted eastward by about 25 m. The major contact between the Tuscan (T) and Ligurian (L) units occurs at an X coordinate value of 36 m.

11

Francese et al., 2007

Geological data in this southern zone was less reliable than in the northern "Aione" site, mainly due to the lack of outcrops. The position of the PFZ was therefore re-mapped on the basis of geophysical evidence.

The "Ripacci" site

The PFZ at this site is a single fault structure (Figure 5b). GPR data represent the only available geophysical information on the "Ripacci" site. Radar signal penetration was generally good, and it was possible to acquire data down to a depth of about 4.0-4.5 m below the topographic surface. We estimated electro-magnetic wave velocities of about 8.0 cm/ns and 9.5 cm/ns in the Ligurian Units and Tuscan Units respectively. Formation velocities were measured directly on nearby outcrops using increasing transmitter-receiver offsets.

Two distinct signatures are clearly visible in the radar profile (Figure 9). The subsurface of the southwestern domain (in the 20-50 m X-coordinate interval) consists of northeast dipping strata with an apparent inclination of 10 degrees (Ligurian Units - L). Reflectivity is much lower in the northeastern domain (in the 50-60 m X-coordinate interval), and the subsurface appears to consist of massive rocks (Tuscan Units - T). The PFZ is imaged as sub-vertical boundaries separating these two domains.

The "Poderino" site

Based on geological data, at the "Poderino" site we expected to find three prominent fault structures belonging to the PFZ (Figures 5c and 6). Major displacement was expected along the middle structure.

In the long ERT-3 profile (Figures 5c and 10) resistivity ranges from 30 ohm*m to 600 ohm*m. In the western segment of the profile, from 210 to 480 m, resistivity values ($\rho < 100$ ohm*m) are typical of clay and shales in the Ligurian Series (L). A horst block with higher resistivity is imaged in the 160-210 m interval; its top is located about 30 m below the surface. This element was interpreted as a sandstone block of the Tuscan series (T) bounded by vertical faults and covered by the conductive layers of the Ligurian Units.

In the short profiles (ERT4, ERT5 and ERT6) resistivity again ranges from 30 ohm*m to more than 500 ohm*m (Figure 10), and two major faults have been clearly imaged. The faults correlate nicely across the profiles, and the low resistivity stripe located respectively at 60 m in profile ERT4 and 51 m in profile ERT5 was interpreted as a highly fractured zone where water circulation occurs. Based on field observations, profile ERT6 should have intersected the centre of the PFZ; in actual fact, it seems to intersect the Ligurian domain (L) alone.

12

Francese et al., 2007

The 3D resistivity volume (Figure 11) covered an area of 115 m x 55 m, and the PFZ was expected to lie approximately in the middle. Resistivity values range from 20 ohm*m in the northwestern zone to more than 150 ohm*m in the southeastern zone.

In the overlapping portion of the 2D profiles and of the 3D measures we observe some slight differences in the overall resistivity values. In general the 3D measures show a lower resistivity as compared to the 2D profiles. A possible reason for this difference is due to the fact that the 3D survey was conducted after several weeks of heavy rainfalls, causing complete water saturation of the subsurface, while the 2D profiles were collected one year earlier during a very dry winter. In addition in the 2D inversion it's assumed that no changes in resistivity occur transversally to the profile direction. This is not true in the study case where the 3D nature of the buried structure affects the apparent resistivity values and the 2D inversion process.

The investigated terrain, in the 3D resistivity volume, exhibits a clear, distinct electric response, and the resistivity distribution is in good agreement with the results of 2D profiles. The clay and shales of the Ligurian domain (L) are fairly conductive, and resistivity is generally lower than 40 ohm*m, whereas the sandstones of the Tuscan domain (T) show resistivity values of 70-100 ohm*m. Some highly resistive near-surface bodies in the western zone correspond to dry quaternary deposits (i.e. gravel and sand). The major contact between the resistive and conductive domains, developing in a northwest-southeast direction, was initially interpreted as the PFZ. At this scale of observation the PFZ has a complex geometry, and the tectonic structure appears to be represented by a west-verging inclined plane with a dip of approximately 45 degrees. A better understanding of the vertical geometry of this plane may be obtained by slicing the volume along a series of YZ planes at various X coordinate values (Figure 12). Near the surface the tectonic contact is almost vertical, while at a 35-40 m depth the dip gradually decreases to 45-30 degrees. This change in dip is probably related both to a local change in the fault plane orientation and to the decrease in signal strength with depth. At present, it is difficult to provide a unique explanation for this low angle contact.

This initial hypothesis of a PFZ locally developed along a NW-SE dipping plane was not satisfactory, and a more detailed analysis of the resistivity volume suggested a slightly different interpretation. The PFZ probably comprises two major sub-vertical faults aligned in a north-south direction (Figure 11) which are connected by a secondary displacement plane with variable dip and orientation. Regionally, the PFZ could therefore be considered a vertical structure locally delimited by a series of variably dipping tectonic contacts.

13

Francese et al., 2007

Three-dimensional electrical imaging suggests that, at a more detailed scale, these tectonic contacts may have a very low dip angle.

According to this new interpretation, the PFZ directions appears to be consistent with the field geology with just a minor westward shift of 10-15 m (Figure 13). The low resistivity zone observed in the 60-100 m Y-coordinate range and for X-coordinates greater than 20 m is still difficult to explain. Although the field geology is based on sparse outcrops, it indicates that the area between the two major faults should be referred to the Tuscan domain. Presently there are two possible explanations: 1) the area falls within the Ligurian (conductive) domain, and the geology needs to be revised; 2) despite its high conductivity, the area is part of the Tuscan domain, and the lowering of resistivity is due to water circulation in a wide fractured zone. The latter hypothesis is also suggested by the occurrence of a well just a few meters north of the profiles and aligned along the nearly N-S strike of the fault.

The unexpected electrical response of the area between the two major faults of the PFZ is also confirmed by the results of the seismic survey (Figure 14).

In the seismic volume there is good differentiation in terms of P-wave velocity. In the Ligurian Units velocity values are generally greater than 2500 m/s, whereas in the Tuscan domains they drop down to less than 2000 m/s.

A depth slice calculated approximately 50 m below the surface clearly reveals two parallel acoustic contacts aligned along a north-south direction, which virtually coincide with geological indications. Elastic wave velocity in the area between the two faults is higher than expected, confirming the anomaly in the resistivity survey and suggesting the presence (at least at depth) of the Ligurian Units.

Although the seismic image has a lower resolution than the resistivity volume, it reveals that the fault planes are almost vertical and that their locations, in agreement with resistivity data, are shifted westwards.

In the southern portion of the seismic volume there is also evidence of an abrupt acoustic contact aligned along a WNW-ESE direction. This contact could be related to a fault plane indicated a few tens of meters further south in the geological map, although this hypothesis is not further supported by other information.

Forward modelling of resistivity data was also utilised to assist data interpretation and devise a first validation tool. We used simple models based on real resistivity values measured directly on the outcrops. Two major drawbacks limited the effectiveness of the forward modelling approach: the electrode spacing

14

Francese et al., 2007

used for the survey was too large to resolve the "core" and the "damage zone" and realistic values for the resistivity of the two zones were not available. Forward modelling results were anyhow usable to confirm the general interpretation framework.

CONCLUSIONS

A multiscale approach based on regional geological investigation, followed by geological field surveys and, lastly, geophysical imaging revealed the structural setting of the "Scansano-Magliano in Toscana" ridge and was used to map the spatial location and buried geometry of the "Patrignone Fault Zone" (PFZ) in detail.

At the various test sites, 2D and 3D resistivity surveying in association with 3D seismic imaging locally resolved the vertical and horizontal contacts between the different geological domains around the PFZ structure with adequate spatial accuracy.

In specific areas of the PFZ structure (especially at the "Poderino" site), the geophysical response revealed the complex geometry of the fracture network previously undetected by surface geological mapping and trench inspections (Figures 11, 12 and 14). We generally observed good agreement between geological and geophysical results, although at the "Poderino" site there are still some uncertainties regarding the area between the two major faults. In this sector, geological data predicted the presence of Tuscan Units, whereas both resistivity and seismic surveys measured parameters typical of the Ligurian Units. Further investigation, by means of trench excavation, is planned to address this point.

The merging of geological and geophysical data helped better define the structural model of the study area. Mainly on the basis of anomalies in rock resistivity values (e.g. Figure 8), we hypothesized that groundwater flows in two zones several meters in thickness on the flanks of the fault core, where the rocks are characterised by the presence of open fractures (*Fd* - fault damaged zone). This idea is supported by the direct observation of the fault in the inspection trenches.

Geophysical results also suggest that the mapped fault planes, almost vertical at the regional scale, could be the envelope of a series of locally high- and low-dipping interconnected planes. Furthermore, the imaged geometry of the fault zones suggests the occurrence of impermeable rocks (i.e. the sandstones of the Macigno Formation) sandwiched between low permeability rocks (i.e. the clays of the Ligurian Units).

15

Francese et al., 2007

A final consideration can be made on the basis of the spatial distribution of the majority of the productive wells. Based on the position of these wells, located very close to the main faults and also on topographic highs (Figure 2a), we formulated a rough conceptual model for water circulation in the Patrignone area (Figure 15). We envisage that a series of fractures generate a staircase structure with alternating permeable and impermeable layers that intercept a regional aquifer at a depth of a few hundred meters. This model could explain the occurrence of water in wells on topographic highs even during the dry seasons (according to the testimony of locals). Preliminary isotopic investigations suggest: i) a common isotopic signature for water samples collected on springs and productive wells located along the PFZ, and ii) the isotopic signature of sampled water is coherent with recharge area at an elevation of about 750-800 m (Mussi et al., 2006). Considering that the maximum elevation along PFZ and surroundings is nearly 600 m, the isotopic data well match the proposed conceptual model for the water circulation in the PFZ (Figure 15). Anyway, we are aware that this is only a preliminary interpretation and that further hydrogeological (e.g. pumping tests) and geochemical (e.g. isotopic and geochemical composition of water) analyses are required to validate and physically constrain the model.

The integrated multiscale study approach was then successfully used to assess the geometry of thin, fractured vertical aquifers in the Apennine zone. The geophysical contribution was essential in developing the subsurface model and in defining the general architecture of the faults. Although the adopted techniques could be used to obtain a sharper image of the fault zone, this was not the primary aim of the present study. The resolution of data obtained during this experiment is adequate for exploration and fault location purposes, and it could be increased by scaling down the acquisition geometry in order to estimate some critical hydraulic parameters. Porosity, permeability and transmissivity, all values that have yet to be determined, must be known in order to effectively plan water exploitation. This issue could be addressed by correlating electrical/seismic data with porosity at specific locations and then generalizing the results. For this reason, future improvements of the study protocol will consist in developing a series of non-invasive geophysical tools capable of estimating these parameters and of assessing water reservoir potentials prior to the drilling of production wells.

16

Francese et al., 2007

This study approach may be easily adapted and exported to other areas where groundwater circulation occurs within fractured aquifers in semi-arid environments of the Mediterranean area.

17

Francese et al., 2007

REFERENCES

Bartole R (1995) The North Tyrrhenian-Northern Apennines post-collisional system: constraints for a geodynamic model. Terra Nova 7:7-30.

Benvenuti G, Brondi M, Dall'Aglio M, Da Roit R, De Cassan P, Ghiara E, Gigli C, Marinelli G, Martini M, Gragnani R, Orlandi C, Paganin G (1971) La Toscana Merdionale: fondamenti geologico minerari per una prospettiva di valorizzazione delle risorse naturali, l'idrologia. Rendiconti della Società Italiana di Mineralogia e Petrologia. 27:211-297.

Bertini G, Costantini A, Cameli GM, Di Filippo M, Decandia FA, Elter FM, Lazzarotto A, Liotta D, Pandeli E, Sandrelli F, Toro B (1991) Struttura geologica dai Monti di Campiglia a Rapolano terme (Toscana meridionale): stato delle conoscenze e problematiche. Studi Geologici Camerti. 1:155-178.

Boccaletti M, Elter P, Guazzone G (1971) Plate tectonics models for the development of Western Alps and Northern Apennines. Nature. 234:108-111.

Bonazzi U, Fazzini P, Gasperi G (1992) Note alla carta geologica del bacino del fiume Albegna. Bollettino della Società Geologica Italiana. 111:341-354.

Bossio A, Costantini A, Lazzarotto A, Liotta D, Mazzanti R, Mazzei R, Salvatorini G, Sandrelli F (1993) Rassegna delle conoscenze sulla stratigrafia del Neoautoctono Toscano. Memorie della Società Geologica Italiana. 49:17-98.

Burgassi PD, Decandia FA, Lazzarotto A (1983) Elementi di stratigrafia e paleogeografia nelle colline metallifere (Toscana) dal Trias al Quaternario. Memorie della Società Geologica Italiana. 25:27-50.

Caine JS, Evans JP, Forster CB (1996) Fault zone architecture and permeability structure. Geology, 24:1025-1028.

Carmignani L, Decandia FA, Disperati L, Fantozzi PL, Lazzarotto A, Liotta D, Oggiano G (1995) Relationships between the Tertiary structural evolution of the Sardinia-Corsica Provencal Domain and the Northern Apennines. Terra Nova. 7:128-137.

Daniels DJ (1996) Surface Penetrating Radar. Institution of Electrical Engineers (IEE). London, UK, 300 pp.

Darcel C, Bour O, Davy P, de Dreuzy JR (2003) Connectivity properties of two-dimensional fracture networks with stochastic fractal correlation. Water Resources Research. 39:1272 DOI:10.1029/2002WR001628.

18

Francese et al., 2007

Decandia FA, Lazzarotto A, Liotta D, Cernobori L, Nicolich R (1998) The CROP 03 traverse: insights on post-collisional evolution of northern Apennines. Memorie della Società Geologica Italiana. 52:427-439.

Demanet D, Pirard E, Renardy F, Jongmans D (2001) Application and processing of geophysical images for mapping faults. Computers & Geosciences. 27:1031-1037.

Innocenti F, Serri G, Ferrara G, Manetti P, Tonarini S (1992) Genesis and classification of the rocks of the Tuscan Magmatic Province: thirty years after Marinelli's model, Acta Vulcanologica. 2:247-265.

Legambiente, (2003) Ecosistema Urbano 2003 di LEGAMBIENTE, Nono Rapporto sulla Qualità Ambientale dei Comuni Capoluogo: a cura di Duccio Bianchi e Lorenzo Bono. Istituto di Ricerche Ambiente Italia. Milano, 18 pp.

Margolin G, Berkowitz B, Scher H (1998) Structure, flow, and generalized conductivity scaling in fracture networks. Water Resources Research. 34: 2103-2121.

Marinelli G, Barberi F, Cioni R (1993) Sollevamenti neogenici e intrusioni acide della Toscana e del Lazio settentrionale. Memorie della Società Geologica Italiana. 49:279-278.

Martelli L, Moratti G, Sani F (1989) Analisi strutturale dei travertini della Toscana meridionale (Valle dell'Albegna). Bollettino della Società Geologica Italiana. 108:197-205.

Mussi M., Doveri M., Calvi E., Catania M., Ferrari E., Giorgi C., Giorgi R. Trifirò S. (2006) Idrogeologia isotopica dei sistemi acquifero ubicati in destra Fiume Albegna nell'area "Magliano in Toscana – Scansano" (relazione finale) - Rapporto Scientifico CNR-IGG n. 10471, convenzione CNR/IGG - ATO6 "Ombrone" del 8/10/2003, 28 pp.

Nguyen F, Garambois S, Jongmans D, Pirard E, Loke, MH (2005) Image processing of 2D resisitivity data for imaging faults. Journal of Applied Geophysics. 57:260-277.

Pasquaré G, Chiesa S, Vezzoli L, Zanchi A (1983) Evoluzione paleogeografica e strutturale di parte della Toscana meridionale a partire dal Miocene Superiore. Memorie della Soicietà Geologica Italiana. 25:145-157.

Porsani JL, Elis VR, Hiodo FY (2005) Geophysical investigation for the characterization of fractured rock aquifers in ITU, SE Brazil. Journal of Applied Geophysics. 57:119-128.

Francese et al., 2007

Serri G, Innocenti F, Manetti P (1993) Geochemical and petrological evidence of the subduction of delaminated Adriatic continental lithosphere in the genesis of the Neogene-Quaternary magmatism of central Italy. Tectonophysics. 223:117-147.

Sharma SP, Baranwal VC (2005) Delineation of groundwater-bearing fracture zones in a hard rock area integrating very low frequency electromagnetic and resistivity data. Journal of Applied Geophysics. 57:155-166.

Schon JH (2004) Physical properties of rocks: Fundamentals and Principles of Petrophysics. In: Helbig K. and Treitel S. (Eds) Handbook of Geophysical Exploration – Seismic Exploration, v18, pp. 583, Elsevier, Amsterdam.

Taylor KC, Minor TC, Chesley MM, Matanawi K (1999) Cost Effectiveness of Well Site Selection Methods in a Fractured Aquifer. Ground Water. 37:271-274.

Wise DJ, Cassidy J, Locke CA (2003) Geophysical imaging of the Quaternary Wairoa North Fault, New Zealand: a case study. Journal of Applied Geophysics. 53:1-16.

Zanchi A, Tozzi M (1987) Evoluzione paleogeografica e strutturale recente del bacino del fiume Albegna (Toscana Meridionale). Geologica Romana. 26:305-325.

20

Francese et al., 2007

FIGURE CAPTIONS AND TABLE HEADINGS
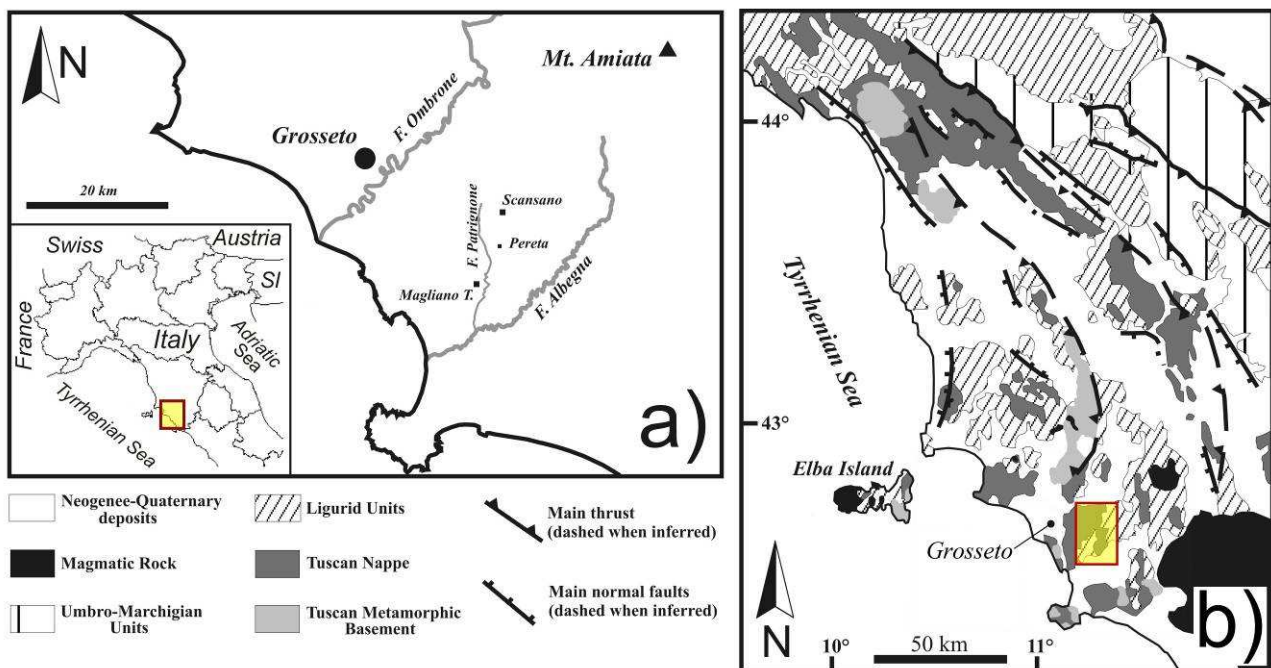
Figure 1.

a) Geographic location of the Scansano-Magliano in Toscana Ridge. b) Geologic sketch map of the studied

area.

Francese et al., 2007
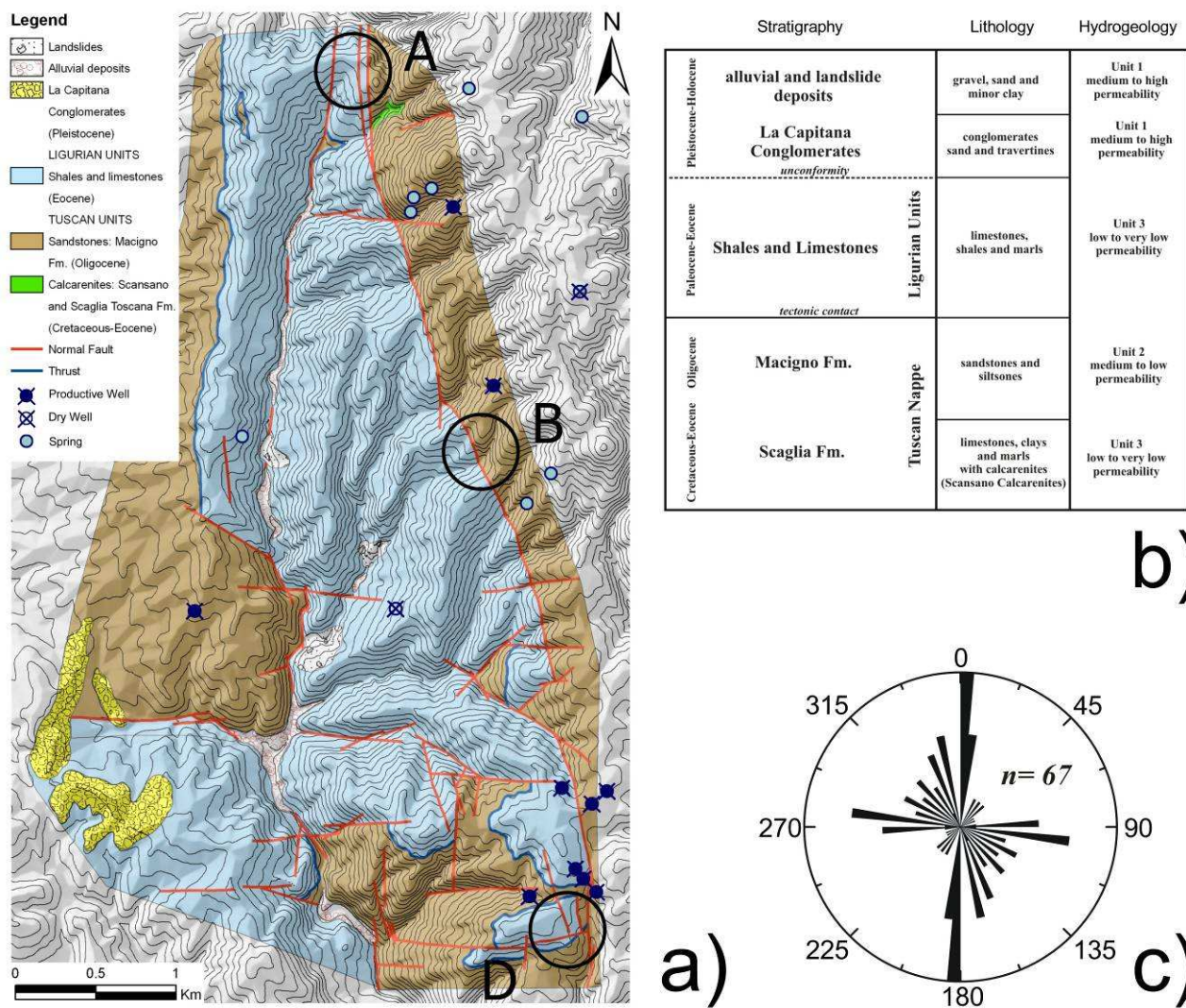
Figure 2.

a) Geologic map of the Patrignone Fault Zone (PFZ). The circles indicate the surveyed sites (see Figure 3).

b) Stratigraphy and hydrogeology of the different units. c) Rose diagram of the frequency distribution of

fractures collected along the PFZ.

Francese et al., 2007
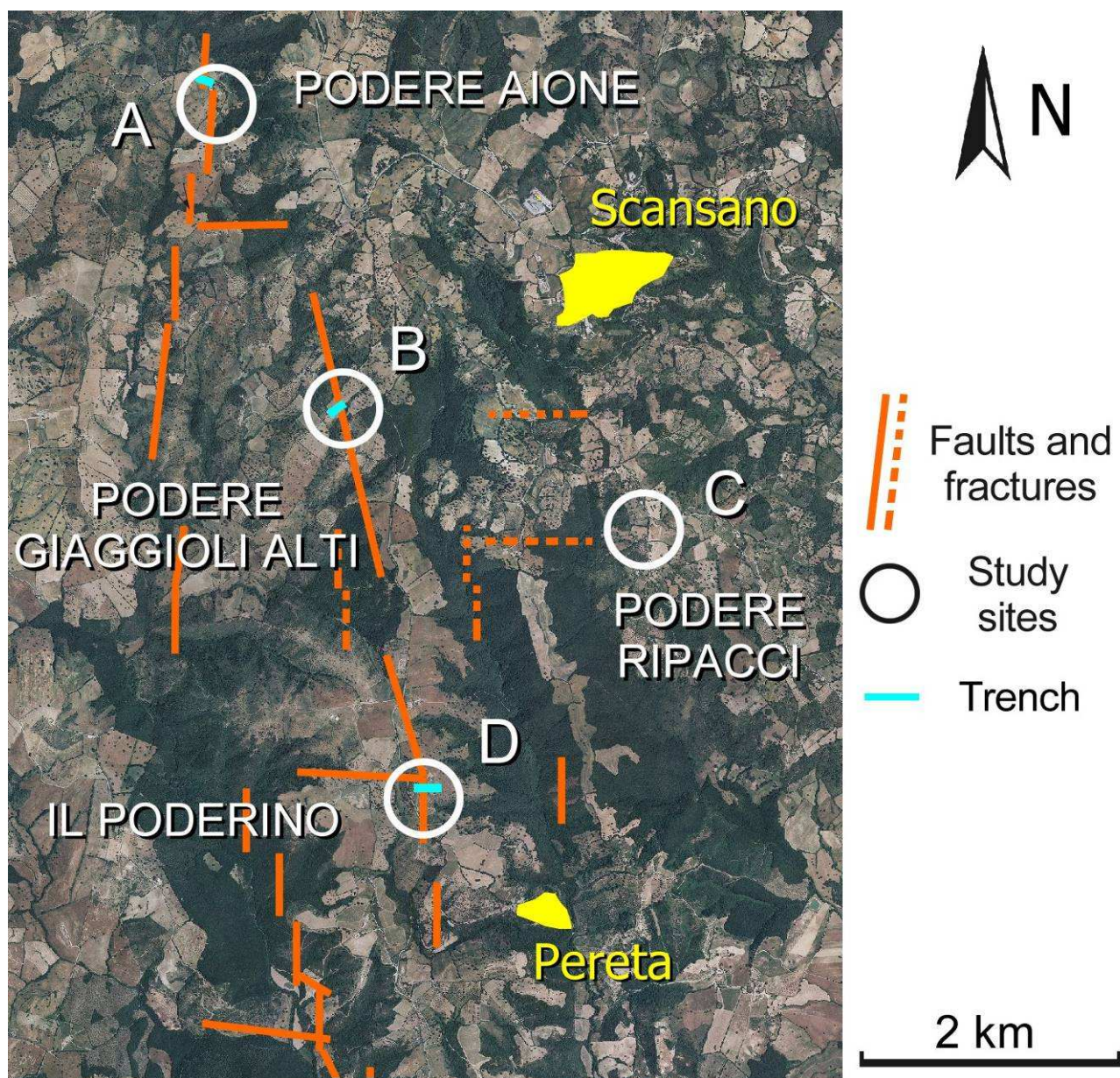
Figure 3.

Distribution of the surveyed sites along the PFZ.

Francese et al., 2007
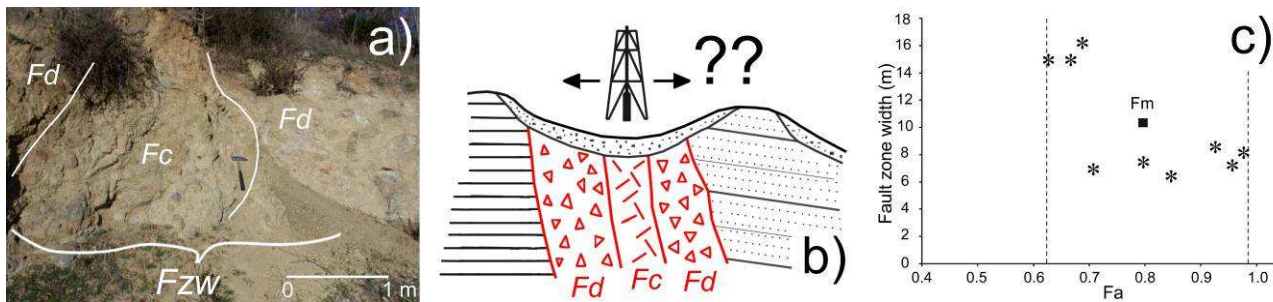
Figure 4.

a) The fault zone (Fzw) consists of a low permeability inner gauge (Fc – fault core) and of the higher permeability flanks (*Fd* – fault damaged zone). b) The spatial position of the fault plane should be mapped in detail in order to successfully drill a fresh water well. c) Diagram of geometric parameters in the Patrignone Fault Zone. Data are listed in Table 2 (asterisks). Fa is the ratio between the width of the damaged zone and the width of the fault zone (see Caine et al., 1996). Fm is the average estimation of Fa. Fs is the difference between maxim and minimum Fa values.
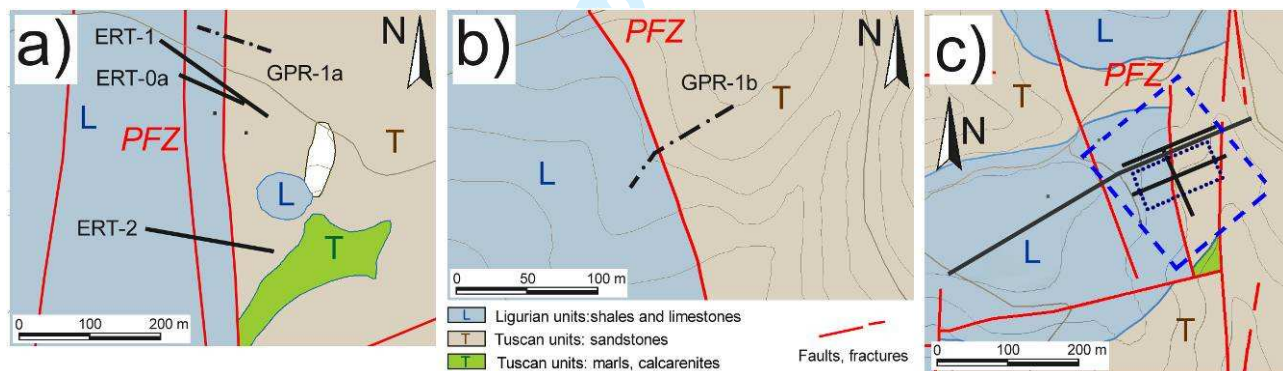
Figure 5.

Geological sketch map showing the location of geophysical investigations at test sites along the PFZ, T - Tuscan units, L - Ligurian units . a) "Aione": three ERT profiles (continuous line): ERT0a, ERT-1 and ERT-2 and a series of GPR profiles (dashed-dotted line); b) "Ripacci": two GPR profiles (dashed-dotted line); c) "Poderino": four ERT profiles (continuous line), a 3D ERT survey (dotted rectangle) and a 3D seismic survey (dashed rectangle), GPR profile location is not shown for clarity.

Francese et al., 2007
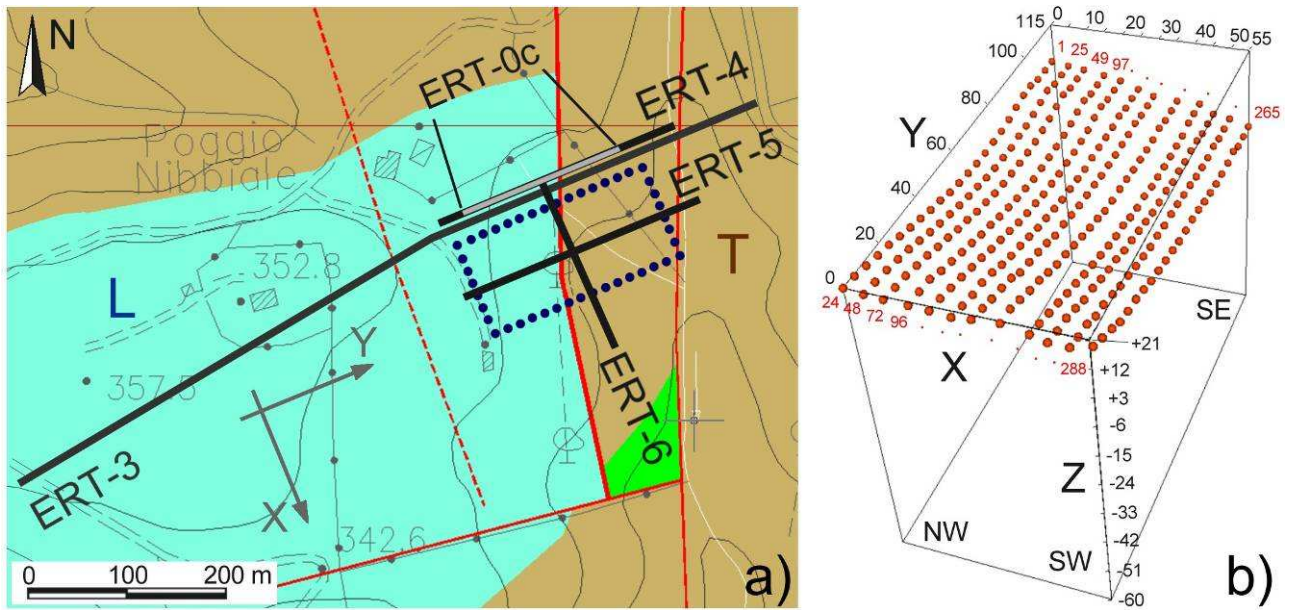
Figure 6.

Geological sketch map of the "Poderino" site and location of the 2D ERT profiles and of the 3D ERT survey

(a) and data acquisition grid for the 3D ERT survey (b). T - Tuscan units, L - Ligurian units.
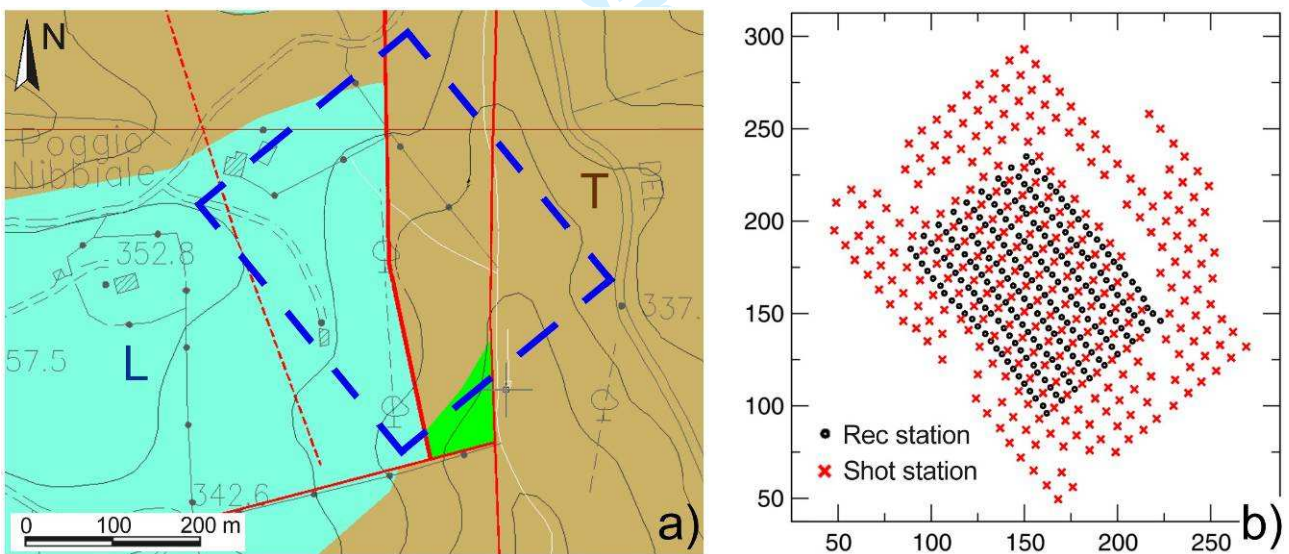
Figure 7.

Geological sketch map of the "Poderino" site and location of the seismic survey across the PFZ (on the left)

and data acquisition grid (on the right). T -Tuscan units, L - Ligurian units.

Francese et al., 2007
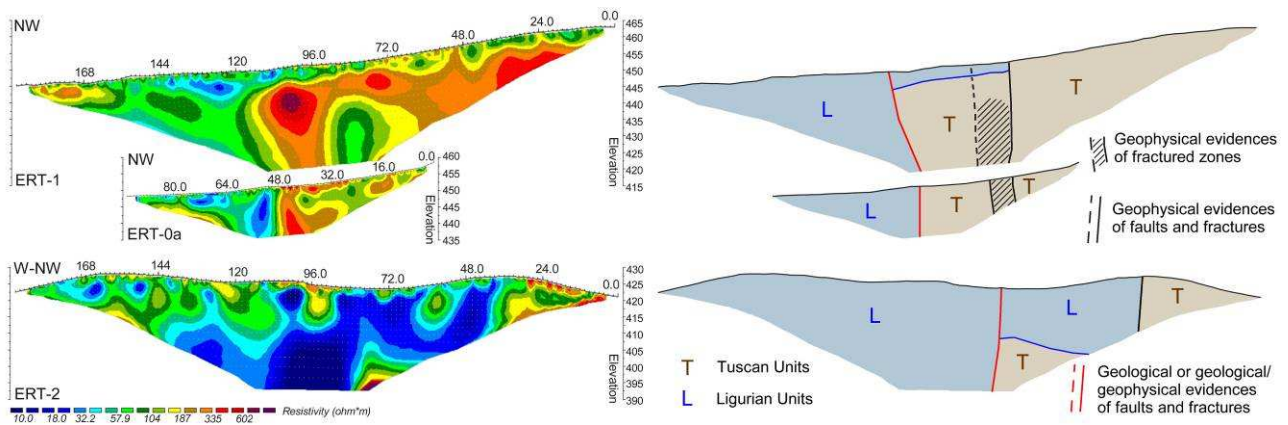
Figure 8.

Resistivity section collected in the "Aione" site (left) and associated interpretation (right). In profiles ERT-1 and ERT-0a there is evidence of a vertical contact between resistive and conductive domains. Geophysical results confirm the existence of two displacement structures, and there is a good agreement between the geological map and the electrical tomography sections regarding the spatial position of PFZ. In profile ERT-2 the geophysical image is not as clear, although two vertical contacts between conductive and resistive domains are visible in the east side of the profile.
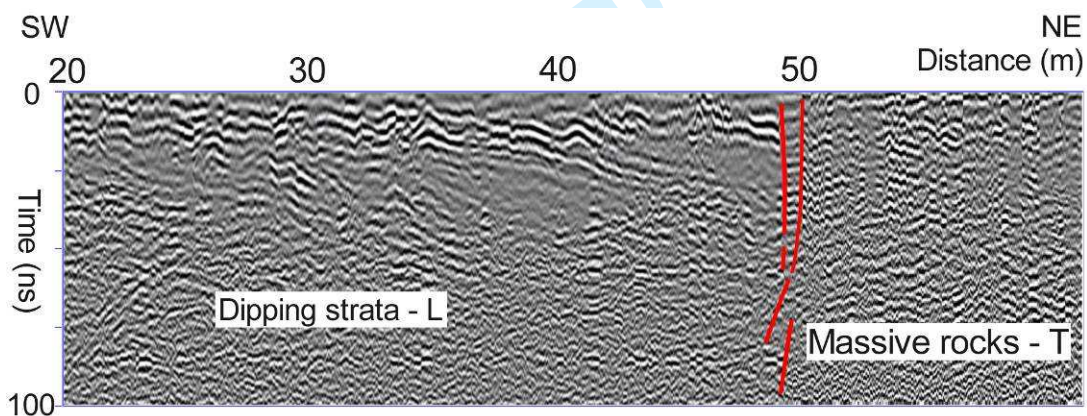
Figure 9.

Inner segment of a typical GPR profile collected in the "Ripacci" site across the PFZ. Two distinct reflectivity signatures are visible in the profile. In the south-western domain (Ligurian Units – L) the radar imaged dipping layered strata while in the north-eastern domain the subsurface appears to be massive (Tuscan Units – T) with no evidences of layering. The PFZ probably marks the boundary between the two domains. The estimated velocity used in the time-to-depth conversion was 8.0 cm/ns and 9.5 cm/ns in the Ligurian Units and Tuscan Units respectively.

26

Francese et al., 2007
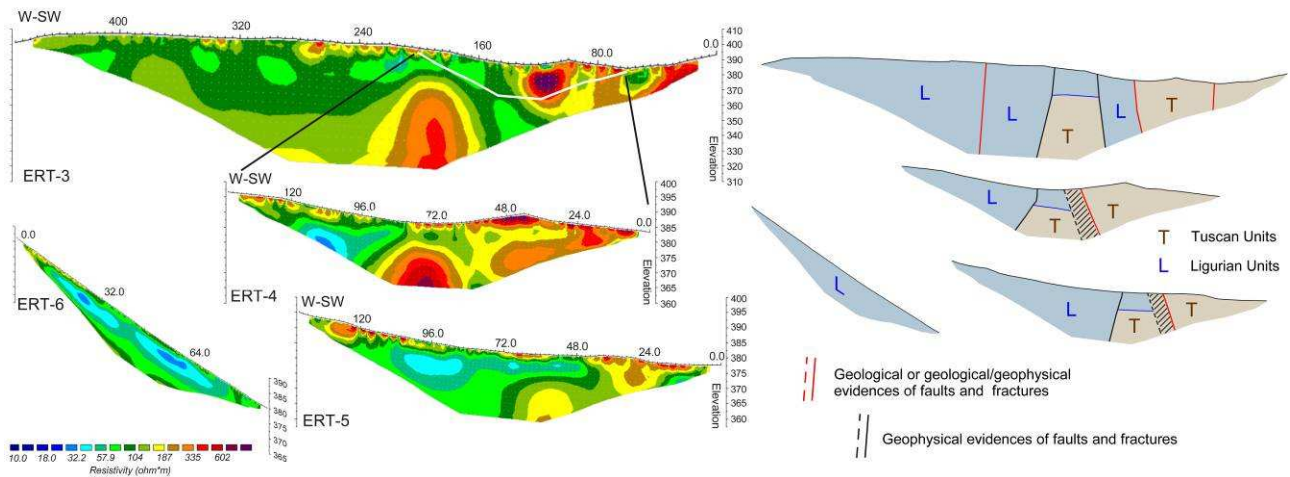
Figure 10.

Resistivity profiles collected in the "Poderino" site (left) and associated interpretation (right). In profile ERT-3, ERT-4 and ERT-5 there are clear evidences of several vertical contacts between resistive and conductive domains. Profile ERT-6, although collected across the PFZ, appears to be entirely within a conductive domain.

Francese et al., 2007
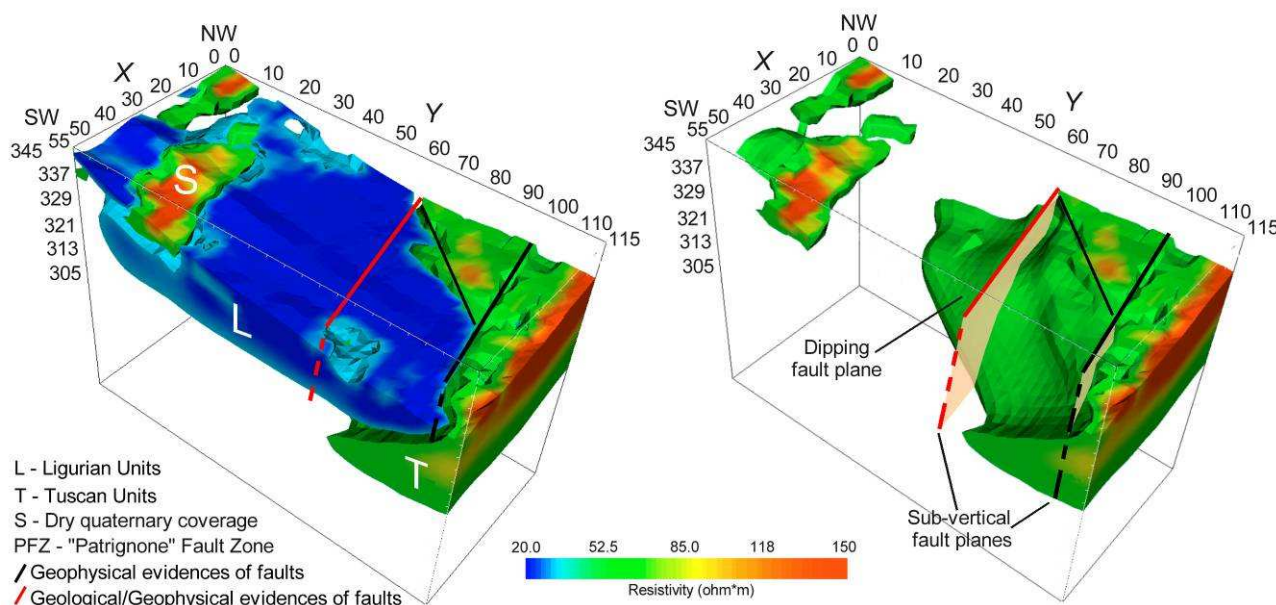
Figure 11.

3D-resistivity volume across the PFZ (left) and extraction of data volume with resistivity values higher than 40 ohm*m (right). The conductive domain (ρ < 40 ohm*m) was associated with the shale lithology of the Ligurian Units (L) while the resistive domain (ρ > 40 ohm*m) was associated to the sandstones of the Tuscan Domain (T). The PFZ appears to be quite complex and comprised of two parallel sub-vertical faults and of a dipping fault.

Francese et al., 2007
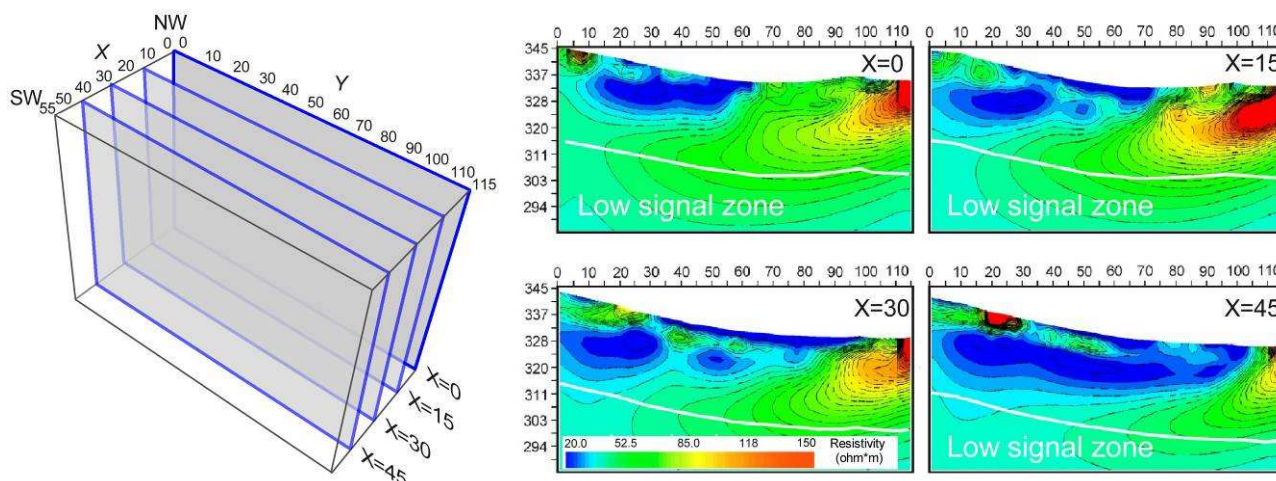
Figure 12.

Series of YZ resistivity planes extracted from the data volume at various values of the Y coordinate. The major contact between the Ligurian and the Tuscan domain appears to progressively shifted eastward and the fault plane seems to lower the angle as the depth increases. The "Low signal zone" in the lower portion of the sections indicates that there are only few data points and that the resistivity image is not as reliable as in the upper segment.

29

Francese et al., 2007
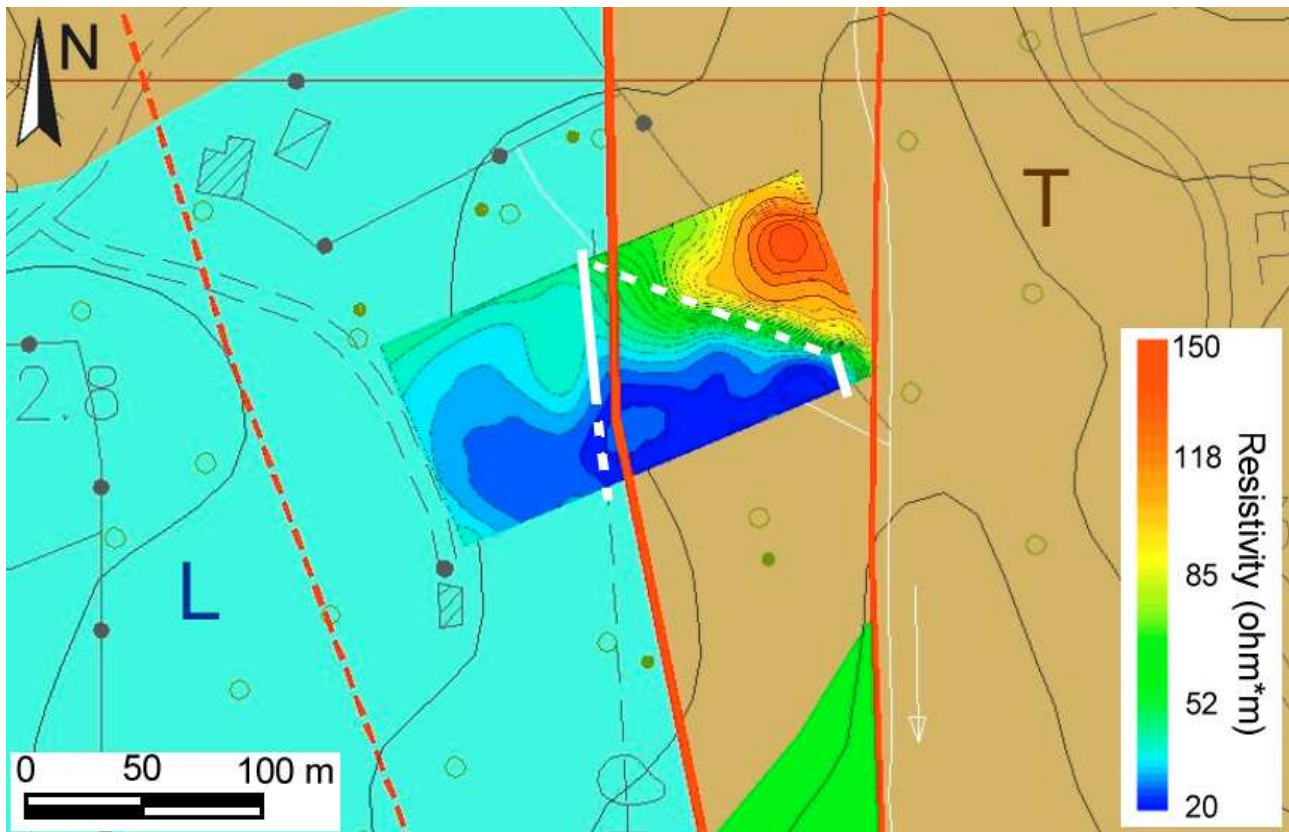
Figure 13.

Resistivity plane (geophysical contacts marked with a white line) extracted from the electrical volume at 320

m of elevation, above sea level, overlaid on the geological map of the site (faults and fractures marked with a

red line). T - Tuscan units, L - Ligurian units.

Francese et al., 2007
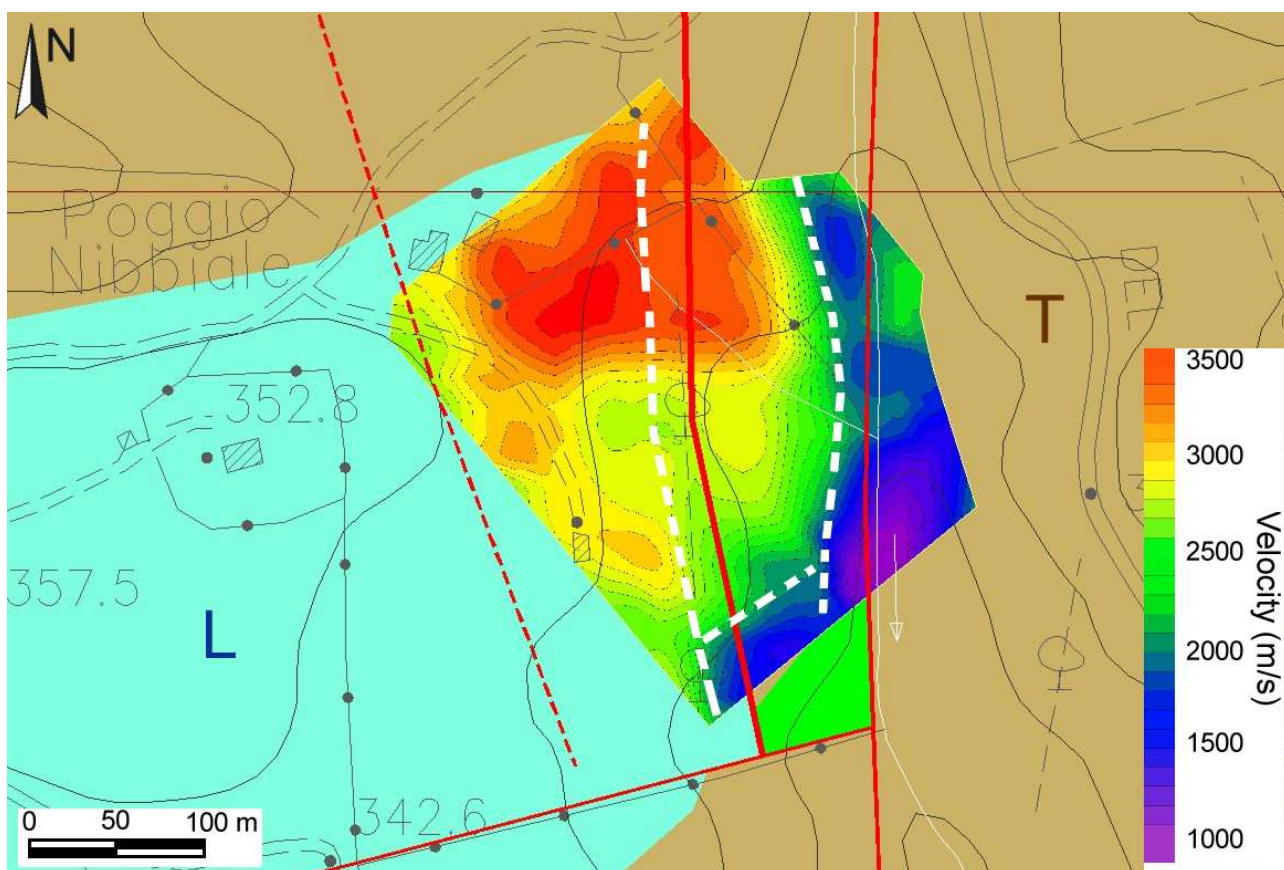
Figure 14.

P-wave velocity plane (geophysical contacts marked with a white line) extracted from the seismic cube at 305 m of elevation, above sea level, overlaid on the geological map of the site (faults and fractures marked with a red line). T - Tuscan units, L - Ligurian units.

31
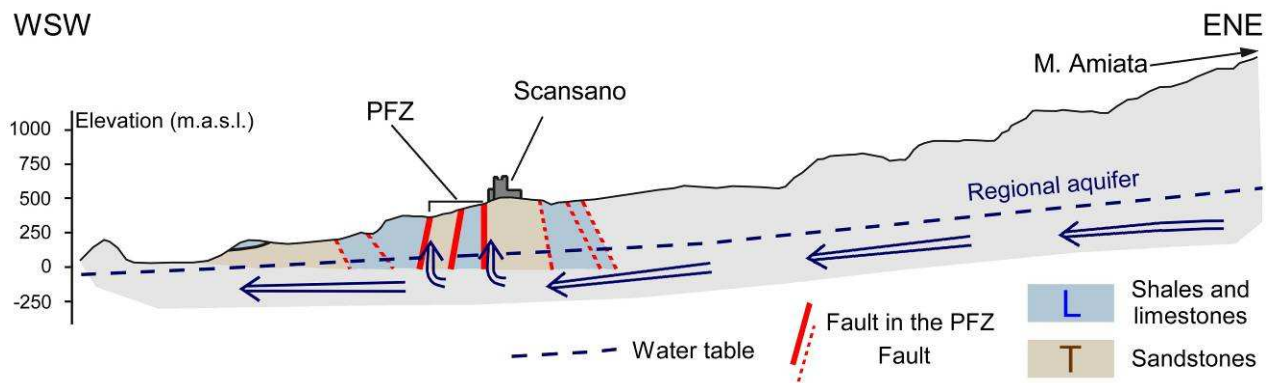
Figure 15.

Conceptual model for water circulation in the Patrignone Fault Zone (PFZ) based on data from the structural and geophysical surveys. Schematic section in which the PFZ faults (thick red lines) separate different blocks of varying lithology. The geology of the area surrounding PFZ is in grey. The dashed blue line approximately delimits the regional aquifer. The arrows indicate the hypothesized flow of groundwater. Note as the water flows into high permeability rocks (sandstone) close to the tectonic contact with low permeability rocks (shale and limestone). The occurrence of a regional aquifer at depth is also suggested by the isotopic composition of water sampled in wells and springs along PFZ (Mussi et al., 2006).

Table 1.

Various sites of investigation along the PFZ

SITE		LITHOLOGY	INVESTIGATION
NAME	CODE		
PODERE AIONE	A	Sandstones, clays and limestones	Trenches and geophysics
PODERE GIAGGIOLI ALTI	B	Clays, limestones and sandstones	Trenches
PODERE RIPACCI	C	Sandstones, clays and marls	Geophysics
IL PODERINO	D	Sandstones, clays and limestones	Trenches and geophysics

Francese et al., 2007

Table 2.

Geometric parameters (according to Caine et al., 1996) computed along the PFZ.

SITE		Fc (m)	Fd (m)	Fa	Fzw (m)	Fm
NAME	CODE					
IL PODERINO	D	0.3	7.0	0.96	7.3	0.95
		0.6	8.0	0.93	8.6	
		0.2	8.0	0.98	8.2	
PODERE GIAGGIOLI ALTI	B	0.3	11.0	0.63	15.0	0.70
		0.6	11.2	0.69	16.2	
		0.2	10.0	0.67	15.0	
PODERE AIONE	A	0.3	5.0	0.71	7.0	0.79
		0.6	6.0	0.80	7.5	
		0.2	5.5	0.85	6.5	

Table 3.

Chronology and details of the geophysical exploration along the PFZ.

		SITE		
	NAME	PODERE AIONE	PODERE RIPACCI	IL PODERINO
	CODE	A	C	D
SURVEY CHRONOLOGY	2003 Autumn	n.1 ERT profile 48 electrodes, 2.0 m spacing (IRIS SYSCAL R1) n.5 GPR profiles (GSSI SIR SYSTEM 2000)	n.2 GPR profiles (GSSI SIR SYSTEM 2000)	n.2 ERT profiles 48 electrodes, 2.0 m spacing (IRIS SYSCAL R1) 64 electrodes, 1.0 m spacing (UNIPD Georesistivimeter) n.10 GPR profiles (GSSI SIR SYSTEM 2000)
	2004 Winter	n.2 ERT profiles 64 electrodes, 3.0 m spacing (UNIPD Georesistivimeter)		n.4 ERT profiles 48 electrodes, 10.0 m, 3.0 m and 2.0 m spacing (IRIS SYSCAL PRO)
	2004 Summer			n.1 3D ERT survey 288 electrodes, 5.0 m x 5.0 m grid size (IRIS SYSCAL PRO)
	2005 Spring			n.1 3D SEISMIC survey 216 channels, 5.0 m x 10 m geophone grid 10.0 m x 10.0 m shot grid (RAS 24 and DMT Compact)